

1 **Title:** Mechanisms of Host Cell Binding and Neurotropism of Zika Virus

2 C.A. Rieder¹, J. Rieder¹, S. Sannajust^{1,2}, D. Goode^{1,2}, R. Geguchadze^{1,2}, R.F. Relich³, D.C. Molliver^{1,2}, T.E.
3 King^{1,2}, J. Vaughn¹, M. May^{1,2*}

4 ¹Department of Biomedical Sciences, College of Osteopathic Medicine, University of New England

5 ²Center for Excellence in the Neurosciences, University of New England

6 ³Department of Pathology and Laboratory Medicine, Indiana University School of Medicine

7

8

9

10

11

12

13

14 **Material Requests and Correspondence should be addressed to:**

15 Meghan May

16 11 Hills Beach Road, 423 Stella Maris Hall, Biddeford, ME USA 04005

17 mmay3@une.edu

18

19 **Keywords:** Zika Virus, Neurotropism, Microcephaly, ASN154, N-acetylglucosamine, Encephalitis, Guillan-
20 Barre syndrome, binding motif

21

22

23

24

25

26 **Abstract:**

27 Zika virus (ZIKV) recently emerged in the Western Hemisphere with previously unrecognized or
28 unreported clinical presentations. Here, we identify two distinct binding mechanisms of ancestral and
29 emergent ZIKV strains featuring the envelope (E) protein residue ASN154 and viral phosphatidylserine
30 (PS). Short (20-mer) peptides representing the region containing ASN154 from strains PRVABC59 (Puerto
31 Rico 2015) and MR_766 (Uganda 1947) were exposed to neuronal cells and fibroblasts, expecting
32 interactions to be representative of ZIKV E protein/cell interactions, and bound MDCK or Vero cells and
33 primary neurons significantly above a scrambled PRVABC59 control peptide. Peptides also significantly
34 inhibited Vero cell adsorption by ZIKV strains MR_766 and PRVABC59, indicating that we have identified
35 a binding mechanism of ancestral African ZIKV strains and emergent Western Hemisphere strains.
36 Pretreatment of ZIKV MR_766 and PRVABC59 with the PS-binding protein annexin V significantly
37 inhibited replication of PRVABC59, but not MR_766, suggesting that Western hemisphere strains are
38 additionally utilizing PS-mediated entry to infect host cells. Taken together, these data indicate that we
39 have identified an ancestral binding mechanism of ZIKV, and a secondary binding mechanism utilized by
40 Western Hemisphere strains.

41

42 **Background**

43 Zika virus (ZIKV) is a mosquito-borne *Flavivirus* that recently emerged and established
44 endemicity in the Western Hemisphere (reviewed here¹⁻²). ZIKV disease historically presented as a mild
45 febrile illness featuring myalgia, rash, and conjunctivitis; however, novel and more severe clinical
46 presentations and increased disease incidence were reported as the virus emerged in the South Pacific³⁻⁴
47 and the Western Hemisphere⁵⁻⁷. Since that time, case reports and animal models have implicated ZIKV in
48 a congenital syndrome most notably featuring microcephaly⁷⁻¹², primary encephalitis, encephalomyelitis,
49 lysencephaly, or Guillan-Barré syndrome^{5, 13-20}, chorioamnionitis²¹, testicular infection²², changes in
50 semen quality²³, and potentially a hemorrhagic shock syndrome²⁴⁻²⁵. The biology and pathogenesis of
51 ZIKV were virtually unexplored at the time of its detection in the Western Hemisphere, making rapid
52 progress toward diagnostics, therapeutics, or vaccine development challenging in the absence of
53 targets²⁶.

54 Substantial progress in the understanding of ZIKV biology has been made in a short time, and
55 includes identification of divergent nucleotide and amino acid sites²⁷⁻³⁰, potential host cell ligands³¹⁻³³,
56 factors that impact replication kinetics³⁴⁻³⁷, and the development of animal models for both
57 neurological and prenatal disease³⁸⁻³⁹. A recent study by Yuan *et al.* demonstrated that a single amino
58 acid substitution within the PrM protein of Western Hemisphere strains conferred increased virulence
59 and resulted in exacerbated pathology *in vivo*³⁷. While this change confers an increased capacity for cell
60 death and correlates with the clinical findings suggesting more severe and invasive disease, it cannot
61 explain the newly emerged ability to directly invade the central nervous system (CNS). We sought to
62 build upon our recent informatics analysis²⁷ by utilizing the findings to identify the binding mechanism of

63 ZIKV. We hypothesized that NAG-glycosylation of E protein ASN154 is linked to ZIKV neuroinvasiveness
64 and that this region plays a critical role in host cell adsorption across strains.

65 **Results and Discussion**

66 ***Binding Motif Prediction***

67 Structural modeling predictions of strain PRVABC59 (Puerto Rico, 2015) indicated that ASN154 is
68 part of a linear β strand (Fig.1A). The disorder probability of this region peaks at 0.72 (Fig.1B), suggesting
69 that this portion of the E protein is particularly dynamic and flexible. Structural and disorder probability
70 predictions of the African type strain MR_766 (Uganda 1947) and the Nigerian strain IbH30656 (Nigeria,
71 1968) exhibit similar characteristics (Fig.1C, D). This region was termed the (putative) Zika virus binding
72 motif (ZVBM).

73 *ZVBM Binding and ZIKV Inhibition*

74 ZVBM sequences from strains PRVABC59, MR_766, and IbH30656 were synthesized and N-
75 terminally labelled with fluorescein isothiocyanate (FITC) (Table 1) in order to assess their capacity to
76 bind ZIKV-susceptible and -permissive cell lines, disrupt ZIKV adsorption, and to interact with dorsal root
77 ganglia (DRG) neurons *ex vivo*. The PRVABC59 sequence was used to generate a peptide that was
78 modified with an NAG molecule at position 8 (equivalent to ASN154), as it natively occurs in this strain,
79 and without carbohydrate modification. ZVBM peptides from MR_766 and PRVABC59 (NAGylated and
80 unglycosylated) all bound Vero cells at levels significantly above those of scrambled PRVABC59
81 (NAGylated and unglycosylated) controls (Fig. 2A, supplemental Fig. S1), suggesting that this motif has
82 the potential to serve as a ZIKV receptor. Binding of the MR_766 ZVBM peptides, despite a four-amino
83 acid deletion relative to PRVABC59, suggests that the critical portion of the ZVBM is potentially
84 contained entirely on the aminoterminal (NTD) or the carboxyterminal (CTD). A peptide representing
85 the NTD of PRVABC59 was unable to bind Vero cells above scrambled control, whereas a peptide
86 representing the CTD bound significantly ($P<0.05$) above the scrambled control, indicating that the
87 putative receptor is contained entirely on the CTD of ZVBM (Fig. 2B). Pretreatment of Vero cell
88 monolayers with the unglycosylated ("Africanized") PRVABC59 ZVBM significantly ($P<0.01$) inhibited
89 infectivity of ZIKV MR_766; conversely, pretreatment of Vero cells with the NAGylated (native)
90 PRVABC59 ZVBM significantly ($P<0.05$) inhibited infectivity of ZIKV PRVABC59 (Fig. 2C, Supplemental
91 Table S1). These findings demonstrate that adherence of ZVBM peptides to Vero cells has functional
92 relevance, and that this motif mediates at least some host cell adsorption.

93 Unglycosylated ZVBM peptides from MR_766 and PRVABC59 bound Madin-Darby Canine Kidney
94 (MDCK) cells significantly ($P<0.05$) above (unglycosylated) scrambled control. Interestingly, NAGylated
95 PRVABC59 did not bind MDCK cells above the NAGylated scrambled control, indicating that functionality
96 of ZVBM as a receptor is host cell-specific (Fig. 2D). Given that MDCK cells are still permissive for ZIKV
97 replication⁴⁰, we hypothesized that a more generalized receptor may be contributing to viral adsorption
98 when ZVBM is NAGylated. The association of human AXL with ZIKV adsorption³¹⁻³³ suggests that viral
99 phosphatidyl serine (PS) may facilitate entry into certain host cells by binding Gas6, which in turn binds
100 AXL, as is seen with multiple viruses⁴¹⁻⁴⁵. We pretreated ZIKV strains MR_766 and PRVABC59 with the

101 PS-binding protein Annexin V prior to infection of Vero cell monolayers. Annexin V significantly ($P<0.05$)
102 inhibited infectivity of PRVABC59 relative to untreated controls (51% reduction) but did not inhibit
103 MR_766 (Fig.2E, Supplemental Table S1), indicating that PS-mediated ZIKV adsorption is possible for
104 ZVBM- NAGylated (*i.e.*, Asian and American lineage) strains. While at least one additional mechanism
105 has been described for the greater infectivity of Asian and American strains³⁷, PS-mediated host cell
106 entry is likely to contribute to this phenotype as well. The capacity of Asian and American lineage strains
107 to utilize at least two binding mechanisms (*i.e.*, PS and ZVBM) suitably explains how AXL can serve as a
108 host cell receptor, but animals who have undergone genetic ablation for *axl* can still serve as permissive
109 hosts for ZIKV⁴⁶⁻⁴⁸.

110 *ZVBM Binding to Neuronal Cells*

111 Disease or infectivity with MR_766 following intrathecal or intracerebral inoculation *in vivo* or
112 neuronal cell infection *in vitro* has been reported⁴⁹⁻⁵³. These findings stand in conflict with a lack of
113 evidence for central nervous system (CNS) involvement during human disease caused by African ZIKV
114 strains. We hypothesized that exposure to neuronal cells *ex vivo* would result in MR_766 ZVBM peptide
115 binding, and the lack of neurological complications during Zika virus disease caused by African strains
116 stems from an inability of these strains to penetrate into the CNS. We collected dorsal root ganglia from
117 C57/black mice and cultured DRG neurons on coverslips. ZVBM peptides from PRVABC59
118 (unglycosylated), MR_766, and IbH30656 were all shown to bind 24-hour DRG neuron cultures by
119 confocal microscopy (Figure 3A-D). Binding was not detected for the scrambled PRVABC59 control
120 peptide. These findings were consistent with those of Annamalai *et al.*, who demonstrated a lack of
121 neurological disease with strains lacking NAGylation at ASN154 when injected intravenously, and overt
122 disease when the same strain was injected intracranially⁵⁴.

123 The outcomes of our *in vitro* and *ex vivo* studies suggest a model of ZIKV neurotropism
124 stemming from NAGylation of the ASN154 facilitating entry into the CNS, wherein binding of certain
125 neuronal cells occurs via the carboxyterminal portion of the ZVBM (*i.e.*, ENRAKV). This model is
126 consistent with both the clinical disparity between ZIKV lineages and the generation of neurological
127 disease by the African strain MR_766 when introduced directly into the CNS as previously described^{37, 50}.
128 Our findings also support previous studies that both implicate AXL as a host cell ligand for
129 Asian/American ZIKV strains and those that show genetically ablated animals are still susceptible to
130 infection by establishing two distinct binding mechanisms for this clade^{31-33, 46-48}. These findings
131 demonstrate the impact of NAGylation of a pathogen surface protein in the vicinity of its binding motif;
132 namely, that there is enhanced potential to penetrate into privileged body sites. This change in
133 posttranslational modification can therefore instantly expand the potential target tissues of infectious
134 agents, and can be expected to similarly expand the array of clinical presentations they cause in turn.

135

136

137

138 **Methods**

139 *Virus Isolates and Culture Conditions.* African Green Monkey Kidney (Vero) cells and Madin-Darby Canine
140 Kidney (MDCK) cells were obtained from the American Type Culture Collection. Cells were routinely
141 propagated in Earle's Minimum Essential Medium (EMEM) with Earle's Balanced Salt Solution,
142 supplemented with 10% fetal bovine serum, L-glutamine and Penicillin/Streptomycin. Cell cultures were
143 incubated at 37°C, with 5% CO₂ and a relative humidity (RH) of 90%. Low-passage isolates of ZIKV strains
144 MR_766 (ATCC VR-84, Uganda) and PRVABC59 (ATCC VR-1843, Puerto Rico) were obtained from the
145 American Type Culture Collection. Virus stocks were propagated on monolayers of Vero cells.
146 Harvested virus lysates were clarified by low-speed centrifugation (500xg/10 min.) and stored in 1-ml
147 aliquots at -80°C.

148

149 *Protein Analysis and Peptide Design.* The Envelope protein structure was visualized using Jmol via the
150 Protein Data Bank (PDB ID 5JHM)⁵⁵⁻⁵⁶, and the PDB Ligand Explorer was used to visualize the structure of
151 N-acetyl glucosamine on ASN154. Probabilities of protein disorder at each amino acid site was
152 estimated using PrDOS⁵⁷. This analysis indicated that the region surrounding ASN154 constitutes a
153 highly disordered linear epitope. Synthetic peptides representing this linear epitope including the
154 differentially glycosylated ASN154 were generated (see Table 1) by Bachem (Bubendorf, Switzerland).
155 The aminoterminal and carboxyterminal domains from PRVABC59 were also synthesized. Peptides were
156 modified by the addition of an aminoterminal FITC label to allow detection and visualization.

157

158 *Primary Dorsal Root (DRG) Ganglia Neuron Culture.* Adult C57/black mice were anesthetized and
159 perfused transcardially with 4°C 1x PBS. Cervical, thoracic and lumbar DRGs were dissected in Ca⁺⁺/Mg⁺⁺-
160 free Hank's basic salt solution (HBSS) and dissociated as previously described⁵⁸. DRGs were cultivated on
161 laminin/polyD-lysine coated EZ slides (MilliporeSigma, Burlington, MA) for 18-24 hours in F-12
162 medium (Gibco, ThermoFisher Scientific, Waltham, MA) supplemented
163 with 10 % fetal bovine serum, 1 % penicillin/streptomycin at 37° C/5% CO₂. Bound peptides were
164 visualized with a Leica TCS SP5 confocal laser scanning microscope.

165

166 *Peptide Binding Assays.* Vero cells and MDCK cells, both of which are permissive for all Zika strains, were
167 grown to 80% confluency in 48-well plates. Following the removal of medium, wells were blocked with
168 10% fetal bovine serum for 30 minutes at 37° C. Peptides (100 µg/mL) were incubated with Vero or
169 MDCK cells for 1 hour at 37° C. Unbound peptides were removed by washing with 1x PBS, and
170 mammalian cells were counterstained with DAPI (diluted 1:300) to control for minor variations in
171 monolayer populations. Bound peptides (FITC) were detected at 485/490 (excitation/emission), and
172 cells were quantified at 350/460. Data are presented as FITC:DAPI ratios. Statistical significance was
173 measured by analyses of variance, and by Fisher's Protected Least Significant Difference test for posthoc
174 comparisons when main effects were significant (GraphPad Prism v. 6.0). Primary DRG neurons grown
175 on coverslips were incubated with 100 µg peptide for 1 hour at 37° C. Unbound peptides were removed
176 by washing with HBSS, and DRG neurons were counterstained with DAPI (diluted 1:300). Bound peptides
177 were visualized using Keyence BZX-700 inverted widefield digital microscope.

178

179 *Viral Adsorption Inhibition Assays by ZVBM Peptides.* Vero cells were propagated in 48-well plates (seed
180 concentration-1e5 cells/well) for 24-hr. Resulting monolayers (85% confluence) were washed twice with
181 warmed PBS and incubated for 2 hours (37° C, 5% CO₂, 90% RH) with 0.1 ml volumes of either PBS
182 (Negative Control), or PBS containing 467 ug of the selected ZVBM peptide. Following treatment, PBS or
183 peptide was decanted, and monolayers washed twice with warmed PBS. ZIKV stocks (stock
184 concentrations: Strain MR_766 – 3.16 e7 TCID₅₀/ml; Strain PRVABC59 – 2e7 TCID₅₀/ml) were serially
185 diluted in serum-free Dulbecco's Minimum Essential Medium (DMEM). Host cell monolayers in treated,
186 or untreated plates were inoculated with either strain MR_766 or PRVABC59 (0.1 ml/well, 5 wells per
187 dilution, N = 3 replicates each) and incubated for 2 hr. After inocula were removed, wells were
188 supplemented with 0.5 ml EMEM growth medium and returned to the incubator. Virus cytopathogenic
189 effects (CPE) were monitored and scored over a period of 10-12 days and the resulting virus titers
190 calculated as TCID₅₀/ml. Statistical significance of changes in virus titer as a result of peptide
191 pretreatment versus untreated control was measured by *Student's* T- test (GraphPad Prism v. 6.0).

192

193 *Virus Treatment with Annexin V.* Annexin V (AbCam, Cambridge, MA) was dissolved in PBS (2335 ug/ml)
194 and filter-sterilized (0.2 um). ZIKV stocks MR_766 and PRVABC59 were then serially diluted in either
195 PBS, or PBS-Annexin V. Dilutions were incubated for 2 hours (37° C, 5% CO₂, 90% RH). Host cell
196 monolayers, prepared in 48-well plates as previously described, were inoculated with respective virus
197 dilutions (0.1 ml/well, 5 wells per dilution, N = 3 replicates each). Virus CPE were scored over a period of
198 10-12 days and the resulting virus titers calculated as TCID₅₀/ml. Statistical significance of changes in
199 virus titer as a result of Annexin V pretreatment versus untreated control was measured by *student's* T
200 test (GraphPad Prism v. 6.0) for each ZIKV strain.

201

202 *Ethical Assurance Statements.* All methods were carried out in accordance with relevant
203 guidelines and regulations. Collection of DRG neurons was performed in accordance with a
204 protocol approved by the University of New England's Institutional Animal Care and Use
205 Committee.

206

207 **Acknowledgements:** This work was supported by intramural awards from the University of New England
208 Center of Excellence for Neuroscience (CEN) an the Office of the Vice President for Research and
209 Scholarship. The authors wish to thank Peter Caradonna (CEN Histology and Imaging Core), Denise
210 Giuvelis (CEN Behavioral Core), and Joshua Havelin for their assistance.

211

212 **Author Contributions:** Peptide motif design and experimentation (CAR, JR, SS); structural and
213 informatics analysis (MM, RFR); neuronal cell extraction development, binding experimentation,

214 confocal imaging parameters (DG, RG, DCM, CAR, SS); viral replication inhibition studies (JV, CAR); Study
215 design, management, execution, and data analysis (MM, RFR, TEK); manuscript preparation (CAR, MM)

216

217 **Additional Information:**

218 *Competing interests*

219 The authors declare no competing interests.

220

221 **References**

- 222 1. Sampathkumar, P. & Sanchez, J. L. Zika Virus in the Americas: A Review for Clinicians. *Mayo Clin.*
223 *Proc.* **91** 514-21 (2016).
- 224 2. Wikan, N. & Smith, D. R. Zika virus: history of a newly emerging arbovirus. *Lancet Infect.*
225 *Dis.* **16** e119-e126, (2016).
- 226 3. Besnard, M., Lastere, S., Teissier, A., Cao-Lormeau, V., & Musso, D. Evidence of perinatal
227 transmission of Zika virus, French Polynesia, December 2013 and February 2014. *Euro. Surveill.* **19**,
228 (2014).
- 229 4. Cauchemez, S., Besnard, M., Bompard, P., Dub, T., Guillemette-Artur, P., Eyrolle-Guignot, D., Salje,
230 H., Van Kerkhove, M. D., Abadie, V., Garel, C., Fontanet, A., & Mallet, H. P. Association between Zika
231 virus and microcephaly in French Polynesia, 2013-15: a retrospective study. *Lancet* **387** 2125-2132,
232 (2016).
- 233 5. Brasil, P., Calvet, G. A., Siqueira, A. M., Wakimoto, M., de Sequeira, P. C., Nobre, A., Quintana, M. e.
234 S., Mendonça, M. C., Lupi, O., de Souza, R. V., Romero, C., Zogbi, H., Bressan, C. a. S., Alves, S. S.,
235 Lourenço-de-Oliveira, R., Nogueira, R. M., Carvalho, M. S., de Filippis, & A. M., Jaenisch, T. Zika Virus
236 Outbreak in Rio de Janeiro, Brazil: Clinical Characterization, Epidemiological and Virological
237 Aspects. *PLoS Negl. Trop. Dis.* **10** e0004636, (2016).
- 238 6. Brasil, P., Sequeira, P. C., Freitas, A. D., Zogbi, H. E., Calvet, G. A., de Souza, R. V., Siqueira, A. M., de
239 Mendonca, M. C., Nogueira, R. M., de Filippis, A. M., & Solomon, T. Guillain-Barré syndrome
240 associated with Zika virus infection. *Lancet* **387** 1482, (2016).
- 241 7. Rasmussen, S. A., Jamieson, D. J., Honein, M. A., & Petersen, L. R. Zika Virus and Birth Defects -
242 Reviewing the Evidence for Causality. *N. Engl. J. Med.* **374** 1981-7, (2016).
- 243 8. de Fatima Vasco Aragao, M., van der Linden, V., Brainer-Lima, A. M., Coeli, R. R., Rocha, M. A., Sobral
244 da Silva, P., Durce Costa Gomes de Carvalho, M., van der Linden, A., Cesario de Holanda, A., &
245 Valenca, M. M. Clinical features and neuroimaging (CT and MRI) findings in presumed Zika virus
246 related congenital infection and microcephaly: retrospective case series study. *BMJ* **353** i1901,
247 (2016).
- 248 9. Mehrjardi, M. Z. Is Zika Virus an Emerging TORCH Agent? An Invited Commentary. *Virology (Auckl)* **8**
249 1178122X17708993, (2017).
- 250 10. Melo, A. S., Aguiar, R. S., Amorim, M. M., Arruda, M. B., Melo, F. O., Ribeiro, S. T., Batista, A. G.,
251 Ferreira, T., Dos Santos, M. P., Sampaio, V. V., Moura, S. R., Rabello, L. P., Gonzaga, C. E., Malinger,

- 252 G., Ximenes, R., de Oliveira-Szejnfeld, P. S., Tovar-Moll, F., Chimelli, L., Silveira, P. P., Delvechio, R.,
253 Higa, L., Campanati, L., Nogueira, R. M., Filippis, A. M., Szejnfeld, J., Voloch, C. M., Ferreira, O. C.,
254 Brindeiro, R. M., & Tanuri, A. Congenital Zika Virus Infection: Beyond Neonatal Microcephaly. *JAMA*
255 *Neurol.* **73** 1407-1416, (2016).
- 256 11. Mlakar, J., Korva, M., Tul, N., Popović, M., Poljšak-Prijatelj, M., Mraz, J., Kolenc, M., Resman Rus, K.,
257 Vesnaver Vipotnik, T., Fabjan Vodusek, V., Vizjak, A., Pižem, J., Petrovec, M., & Avšič Županc, T. Zika
258 Virus Associated with Microcephaly. *N. Engl. J. Med.* **374** 951-8, (2016).
- 259 12. Reynolds, M. R., Jones, A. M., Petersen, E. E., Lee, E. H., Rice, M. E., Bingham, A., Ellington, S. R.,
260 Evert, N., Reagan-Steiner, S., Oduyebo, T., Brown, C. M., Martin, S., Ahmad, N., Bhatnagar, J.,
261 Macdonald, J., Gould, C., Fine, A. D., Polen, K. D., Lake-Burgher, H., Hillard, C. L., Hall, N., Yazdy, M. M.,
262 Slaughter, K., Sommer, J. N., Adamski, A., Raycraft, M., Fleck-Derderian, S., Gupta, J., Newsome, K.,
263 Baez-Santiago, M., Slavinski, S., White, J. L., Moore, C. A., Shapiro-Mendoza, C. K., Petersen, L.,
264 Boyle, C., Jamieson, D. J., Meaney-Delman, D., & Honein, M. A., Collaboration, U. S. Z. P. R. Vital
265 Signs: Update on Zika Virus-Associated Birth Defects and Evaluation of All U.S. Infants with
266 Congenital Zika Virus Exposure - U.S. Zika Pregnancy Registry, 2016. *MMWR Morb. Mortal. Wkly.*
267 *Rep.* **66** 366-373, (2017).
- 268 13. Acevedo, N., Waggoner, J., Rodriguez, M., Rivera, L., Landivar, J., Pinsky, B., & Zambrano, H. Zika
269 Virus, Chikungunya Virus, and Dengue Virus in Cerebrospinal Fluid from Adults with Neurological
270 Manifestations, Guayaquil, Ecuador. *Front. Microbiol.* **8** doi: 10.3389/fmicb.2017.00042. eCollection
271 2017 (2017).
- 272 14. De Broucker, T., Mailles, A., & Stahl, J. P. Neurological Presentation of Zika Virus Infection Beyond
273 the Perinatal Period. *Curr. Infect. Dis. Rep.* **19** 35 (2017).
- 274 15. Dub, T. & Fontanet, A. Zika virus and Guillain-Barré syndrome. *Rev. Neuro.l (Paris)* **173** 361-363
275 (2017).
- 276 16. Galliez, R. M., Spitz, M., Rafful, P. P., Cagy, M., Escosteguy, C., Germano, C. S., Sasse, E., Gonçalves,
277 A. L., Silveira, P. P., Pezzuto, P., Ornelas, A. M., Tanuri, A., Aguiar, R. S., & Moll, F. T. Zika Virus
278 Causing Encephalomyelitis Associated With Immunoactivation. *Open Forum Infect. Dis.* **3** ofw203,
279 (2016).
- 280 17. Roth, W., Tyshkov, C., Thakur, K., & Vargas, W. Encephalomyelitis Following Definitive Zika Virus
281 Infection. *Neurol Neuroimmunol Neuroinflamm* **4** e349, (2017).
- 282 18. Rozé, B., Najioullah, F., Signate, A., Apetse, K., Brouste, Y., Gourgoudou, S., Fagour, L., Abel, S.,
283 Hochedez, P., Cesaire, R., Cabié, A., & the Martinique Neuro-Zika Working Group. Zika virus
284 detection in cerebrospinal fluid from two patients with encephalopathy, Martinique, February
285 2016. *Euro. Surveill.* **21** doi: 10.2807/1560-7917.ES.2016.21.16.30205, (2016).
- 286 19. Thiery, G., Valentino, R., & Meddhaoui, H. Zika virus-associated Guillain-Barré syndrome: a warning
287 for critical care physicians. *Intensive Care Med.* **42** 1485-6, (2016).
- 288 20. Zare Mehrjardi, M., Keshavarz, E., Poretti, A., Hazin, A. N. Neuroimaging findings of Zika virus
289 infection: a review article. *Jpn J Radiol* **34** 765-770 (2016).
- 290 21. Rosenberg, A. Z., Yu, W., Hill, D. A., Reyes, C. A., & Schwartz, D. A. Placental Pathology of Zika Virus:
291 Viral Infection of the Placenta Induces Villous Stromal Macrophage (Hofbauer Cell) Proliferation and
292 Hyperplasia. *Arch. Pathol. Lab Med.* **141** 43-48, (2017).

- 293 22. Ma, W., Li, S., Ma, S., Jia, L., Zhang, F., Zhang, Y., Zhang, J., Wong, G., Zhang, S., Lu, X., Liu, M., Yan, J.,
294 Li, W., Qin, C., Han, D., Wang, N., Li, X., & Gao, G. F. Zika Virus Causes Testis Damage and Leads to
295 Male Infertility in Mice. *Cell* **167** 1511-1524.e10, (2016).
- 296 23. Jogueux, G., Mansuy, J. M., Matusali, G., Hamdi, S., Walschaerts, M., Pavili, L., Guyomard, S., Prisant,
297 N., Lamarre, P., Dejucq-Rainsford, N., Pasquier, C., & Bujan, L. Effect of acute Zika virus infection on
298 sperm and virus clearance in body fluids: a prospective observational study. *Lancet Infect. Dis.* **17**
299 1200-1208 (2017).
- 300 24. Brent, C., Dunn, A., Savage, H., Faraji, A., Rubin, M., Risk, I., Garcia, W., Cortese, M., Novosad, S.,
301 Krow-Lucal, E. R., Crain, J., Hill, M., Atkinson, A., Peterson, D., Christensen, K., Dimond, M., Staples, J.
302 E., & Nakashima, A. Preliminary Findings from an Investigation of Zika Virus Infection in a Patient
303 with No Known Risk Factors - Utah, 2016. *MMWR Morb. Mortal. Wkly. Rep.* **65** 981-2, (2016).
- 304 25. Zonneveld, R., Roosblad, J., Staveren, J. W., Wilschut, J. C., Vreden, S. G., & Codrington, J. Three
305 atypical lethal cases associated with acute Zika virus infection in Suriname. *ID Cases* **5** 49-53 (2016).
- 306 26. Relich, R. F. & Loeffelholz, M. Zika Virus. *Clin Lab Med* **37** 253-267, (2017).
- 307 27. May, M. & Relich, R. F. A Comprehensive Systems Biology Approach to Studying Zika Virus. *PLoS*
308 *One* **11** e0161355, (2016).
- 309 28. Faye, O., Freire, C. C., Iamarino, A., de Oliveira, J. V., Diallo, M., Zanotto, P. M., & Sall, A. A. Molecular
310 evolution of Zika virus during its emergence in the 20(th) century. *PLoS Negl. Trop. Dis.* **8** e2636,
311 (2014).
- 312 29. Lanciotti, R. S., Lambert, A. J., Holodniy, M., Saavedra, S., & Signor, L. e. C. Phylogeny of Zika Virus in
313 Western Hemisphere, 2015. *Emerg. Infect. Dis.* **22** 933-5, (2016).
- 314 30. Zhu, Z., Chan, J. F., Tee, K. M., Choi, G. K., Lau, S. K., Woo, P. C., Tse, H., & Yuen, K. Y. Comparative
315 genomic analysis of pre-epidemic and epidemic Zika virus strains for virological factors potentially
316 associated with the rapidly expanding epidemic. *Emerg. Microbes Infect.* **5** e22, (2016).
- 317 31. Liu, S., DeLalio, L. J., Isakson, B. E., & Wang, T. T. AXL-Mediated Productive Infection of Human
318 Endothelial Cells by Zika Virus. *Circ. Res.* **119** 1183-1189, (2016).
- 319 32. Nowakowski, T. J., Pollen, A. A., Di Lullo, E., Sandoval-Espinosa, C., Bershteyn, M., & Kriegstein, A. R.
320 Expression Analysis Highlights AXL as a Candidate Zika Virus Entry Receptor in Neural Stem Cells. *Cell*
321 *Stem Cell* **18** 591-6 (2016).
- 322 33. Richard, A. S., Shim, B. S., Kwon, Y. C., Zhang, R., Otsuka, Y., Schmitt, K., Berri, F., Diamond, M. S., &
323 Choe, H. AXL-dependent infection of human fetal endothelial cells distinguishes Zika virus from
324 other pathogenic flaviviruses. *Proc. Natl. Acad. Sci. USA* **114** 2024-2029, (2017).
- 325 34. Bardina, S. V., Bunduc, P., Tripathi, S., Duehr, J., Frere, J. J., Brown, J. A., Nachbagauer, R., Foster, G.
326 A., Kryzstof, D., Tortorella, D., Stramer, S. L., Garcia-Sastre, A., Krammer, F., & Lim, J. K.
327 Enhancement of Zika virus pathogenesis by preexisting ant flavivirus immunity. *Science* **356**, 175-180
328 (2017).
- 329 35. Castanha, P. M. S., Nascimento, E. J. M., Braga, C., Cordeiro, M. T., de Carvalho, O. V., de Mendonça,
330 L. R., Azevedo, E. A. N., França, R. F. O., Dhalia, R., & Marques, E. T. A. Dengue Virus-Specific
331 Antibodies Enhance Brazilian Zika Virus Infection. *J. Infect. Dis.* **215** 781-785, (2017).
- 332 36. Paul, L. M., Carlin, E. R., Jenkins, M. M., Tan, A. L., Barcellona, C. M., Nicholson, C. O., Michael, S. F.,
333 & Isern, S. Dengue virus antibodies enhance Zika virus infection. *Clin. Transl. Immunology* **5** e117,
334 (2016).

- 335 37. Yuan, L., Huang, X. Y., Liu, Z. Y., Zhang, F., Zhu, X. L., Yu, J. Y., Ji, X., Xu, Y. P., Li, G., Li, C., Wang, H. J.,
336 Deng, Y. Q., Wu, M., Cheng, M. L., Ye, Q., Xie, D. Y., Li, X. F., Wang, X., Shi, W., Hu, B., Shi, P. Y., Xu, Z.,
337 & Qin, C. F. A single mutation in the prM protein of Zika virus contributes to fetal
338 microcephaly. *Science* **358** 933-936 (2017).
- 339 38. Dowall, S. D., Graham, V. A., Rayner, E., Atkinson, B., Hall, G., Watson, R. J., Bosworth, A., Bonney, L.
340 C., Kitchen, S., & Hewson, R. A Susceptible Mouse Model for Zika Virus Infection. *PLoS Negl. Trop.*
341 *Dis.* **10** e0004658, (2016).
- 342 39. Koide, F., Goebel, S., Snyder, B., Walters, K. B., Gast, A., Hagelin, K., Kalkeri, R., & Rayner, J.
343 Development of a Zika Virus Infection Model in Cynomolgus Macaques. *Front. Microbiol.* **7** 2028
344 (2016).
- 345 40. Barr, K. L., Anderson, B. D., Prakoso, D., Long, M. T. Working with Zika and Usutu Viruses In
346 Vitro. *PLoS Negl. Trop. Dis.* **10** e0004931, (2016).
- 347 41. Carnec, X., Meertens, L., Dejarnac, O., Perera-Lecoin, M., Hafirassou, M. L., Kitauro, J., Ramdasi, R.,
348 Schwartz, O., & Amara, A. The Phosphatidylserine and Phosphatidylethanolamine Receptor CD300a
349 Binds Dengue Virus and Enhances Infection. *J. Virol.* **90** 92-102, (2015).
- 350 42. Jemielity, S., Wang, J. J., Chan, Y. K., Ahmed, A. A., Li, W., Monahan, S., Bu, X., Farzan, M., Freeman,
351 G. J., Umetsu, D. T., Dekruyff, R. H., & Choe, H. TIM-family proteins promote infection of multiple
352 enveloped viruses through virion-associated phosphatidylserine. *PLoS Pathog.* **9** e1003232 (2013).
- 353 43. Meertens, L., Labeau, A., Dejarnac, O., Cipriani, S., Sinigaglia, L., Bonnet-Madin, L., Le Charpentier, T.,
354 Hafirassou, M. L., Zamborlini, A., Cao-Lormeau, V. M., Couplier, M., Missé, D., Jouvenet, N.,
355 Tabibiazar, R., Gressens, P., Schwartz, O., & Amara, A. Axl Mediates ZIKA Virus Entry in Human Glial
356 Cells and Modulates Innate Immune Responses. *Cell Rep.* **18** 324-333, (2017).
- 357 44. Richard, A. S., Zhang, A., Park, S. J., Farzan, M., Zong, M., & Choe, H. Virion-associated
358 phosphatidylethanolamine promotes TIM1-mediated infection by Ebola, dengue, and West Nile
359 viruses. *Proc. Natl. Acad. Sci. USA* **112** 14682-7 (2015).
- 360 45. Wang, J., Qiao, L., Hou, Z., & Luo, G. TIM-1 Promotes Hepatitis C Virus Cell Attachment and
361 Infection. *J. Virol.* **91** e01583-16, (2017).
- 362 46. Hastings, A. K., Yockey, L. J., Jagger, B. W., Hwang, J., Uraki, R., Gaitsch, H. F., Parnell, L. A., Cao, B.,
363 Mysorekar, I. U., Rothlin, C. V., Fikrig, E., Diamond, M. S., & Iwasaki, A. TAM Receptors Are Not
364 Required for Zika Virus Infection in Mice. *Cell Rep.* **19** 558-568, (2017).
- 365 47. Li, F., Wang, P. R., Qu, L. B., Yi, C. H., Zhang, F. C., Tang, X. P., Zhang, L. G., & Chen, L. AXL is not
366 essential for Zika virus infection in the mouse brain. *Emerg. Microbes Infect.* **6** e16, (2017).
- 367 48. Wells, M. F., Salick, M. R., Wiskow, O., Ho, D. J., Worringer, K. A., Ihry, R. J., Kommineni, S., Bilican,
368 B., Klim, J. R., Hill, E. J., Kane, L. T., Ye, C., Kaykas, A., & Eggan, K. Genetic Ablation of AXL Does Not
369 Protect Human Neural Progenitor Cells and Cerebral Organoids from Zika Virus Infection. *Cell Stem*
370 *Cell* **19** 703-708, (2016).
- 371 49. Duggal, N. K., Ritter, J. M., McDonald, E. M., Romo, H., Guirakhoo, F., Davis, B. S., Chang, G. J., &
372 Brault, A. C. Differential Neurovirulence of African and Asian Genotype Zika Virus Isolates in Outbred
373 Immunocompetent Mice. *Am. J. Trop. Med. Hyg.* **97** 1410-1417, (2017).
- 374 50. Li, C., Xu, D., Ye, Q., Hong, S., Jiang, Y., Liu, X., Zhang, N., Shi, L., Qin, C. F., & Xu, Z. Zika Virus Disrupts
375 Neural Progenitor Development and Leads to Microcephaly in Mice. *Cell Stem Cell* **19** 120-6 (2016).

- 376 51. Shao, Q., Herrlinger, S., Yang, S. L., Lai, F., Moore, J. M., Brindley, M. A., & Chen, J. F. Zika virus
377 infection disrupts neurovascular development and results in postnatal microcephaly with brain
378 damage. *Development* **143** 4127-4136, (2016).
- 379 52. Shao, Q., Herrlinger, S., Zhu, Y. N., Yang, M., Goodfellow, F., Stice, S. L., Qi, X. P., Brindley, M. A., &
380 Chen, J. F. The African Zika virus MR-766 is more virulent and causes more severe brain damage
381 than current Asian lineage and dengue virus. *Development* **144** 4114-4124, (2017).
- 382 53. Tang, H., Hammack, C., Ogden, S. C., Wen, Z., Qian, X., Li, Y., Yao, B., Shin, J., Zhang, F., Lee, E. M.,
383 Christian, K. M., Didier, R. A., Jin, P., Song, H., & Ming, G. L. Zika Virus Infects Human Cortical Neural
384 Progenitors and Attenuates Their Growth. *Cell Stem Cell* **18** 587-90, (2016).
- 385 54. Annamalai, A. S., Pattnaik, A., Sahoo, B. R., Muthukrishnan, E., Natarajan, S. K., Steffen, D., Vu, H. L.
386 X., Delhon, G., Osorio, F. A., Petro, T. M., Xiang, S. H., & Pattnaik, A. K. Zika Virus Encoding Non-
387 Glycosylated Envelope Protein is Attenuated and Defective in Neuroinvasion. *J. Virol.* doi:
388 10.1128/JVI.01348-17. (2017).
- 389 55. Berman, H. M., Bhat, T. N., Bourne, P. E., Feng, Z., Gilliland, G., Weissig, H., & Westbrook, J. The
390 Protein Data Bank and the challenge of structural genomics. *Nat. Struct. Biol.* **7**, 957-9 (2000).
- 391 56. Dai, L., Song, J., Lu, X., Deng, Y. Q., Musyoki, A. M., Cheng, H., Zhang, Y., Yuan, Y., Song, H., Haywood,
392 J., Xiao, H., Yan, J., Shi, Y., Qin, C. F., Qi, J., & Gao, G. F. Structures of the Zika Virus Envelope Protein
393 and Its Complex with a Flavivirus Broadly Protective Antibody. *Cell Host Microbe* **19** 696-704, (2016).
- 394 57. Ishida, T. & Kinoshita, K. PrDOS: prediction of disordered protein regions from amino acid
395 sequence. *Nucleic Acids Res.* **35** W460-4, (2007).
- 396 58. Malin, S. A., Davis, B. M., Molliver, D. C. Production of dissociated sensory neuron cultures and
397 considerations for their use in studying neuronal function and plasticity. *Nat. Protoc.* **2** 152-60,
398 (2007).

399

400

401

402

403

404

405

406

407

408

409

410

411

412 Table 1: Peptide Sequences

Peptide Name ^a	Sequence ^b	Strain Type ^c
PRVABC59-N	*QHSGMIV ^N DTGHETDENRAKV	Asian/American
PRVABC59	*QHSGMIVNDTGHETDENRAKV	“African”
MR_766	*QHSGMI----GYETDENRAKV	African
IbH30656	*QHSGMIVND-----ENRAKV	African
Scrambled	*QDHVIHVDMTGRTGSEEANKN	N/A
Scrambled-N	*QDHVIHVDMTGRTGSEEAN ^N KN	N/A
PRVABC59-NTD	*QHSGMIVND	“African” partial
PRVABC59-CTD	*ENRAKV	Asian/American

413 ^aPeptides are named for the strain they derived from. The modifiers N, NTD, and CTD reflect the
414 addition of NAG, use of the aminoterminal domain, or the carboxyterminal domain, respectively.

415 ^bAsterisk (*) indicate location of the FITC molecule. Shaded asparagine (N) residues indicate location of
416 NAG coupling.

417 ^cThe designation “African” indicates that sequence from the Asian/American clade strain PRVABC59 has
418 been made to resemble an African strain by its lack of NAG.

419

420

421

422

423

424

425 **Figures and Figure Legends**

426 **Figure 1: Envelope Protein Structure.** (A) The predicted E protein structure indicates that the region
427 containing ASN154 (circled) and its NAG modification (inset) is a linear β strand. Intrinsic disorder
428 probabilities were calculated for each amino acid position in the E protein sequence from strains (B)
429 PRVABC59, (C) MR_766, and (D) IbH30656. Probabilities above 0.5 (blue line) are considered indicative
430 of sites representing disordered regions. The region containing ASN154 is indicated (blue box) for each
431 strain.

432

433 **Figure 2: ZVBM Binding and ZIKV Inhibition.** (A) NAGylated or unglycosylated ZVBM peptides from
434 strain PRVABC59 and the type strain MR_766 bound Vero cells significantly (* $P < 0.05$) above scrambled
435 ZVBM sequences from PRVABC59, with or without NAG modification. (B) A shorter peptide representing
436 the NTD of PRVABC59 was unable to bind Vero cells above the full-length ZVBM scrambled control;
437 however, a peptide representing the CTD bound Vero cells at a significantly (** $P < 0.01$) higher level than
438 the NTD or scrambled control. (C) Pretreatment of Vero cells with unglycosylated ZVBM peptide
439 (PRVABC59) significantly (* $P < 0.05$) inhibited ZIKV MR_766 replication relative to untreated controls,
440 whereas the unglycosylated scrambled control peptide was not. Similarly, pretreatment with NAGylated
441 ZVBM peptide (PRVABC59) significantly (** $P < 0.01$) inhibited ZIKV PRVABC59 replication relative to
442 untreated controls, whereas the NAGylated scrambled control peptide was not. (D) Unglycosylated
443 PRVABC59 and MR_766 ZVBM peptides bound MDCK cells significantly (* $P < 0.05$) above unglycosylated
444 or NAGylated scrambled controls; however, the NAGylated PRVABC59 ZVBM peptide was not. (E)
445 Pretreatment of ZIKV strain PRVABC59 with annexin V significantly (** $P < 0.01$) inhibited viral replication
446 on Vero cells relative to untreated controls, whereas replication of ZIKV MR_766 following pretreatment
447 with annexin V was unaffected.

448

449 **Figure 3: Peptide binding to DRG Neurons *ex vivo*.** Primary DRG neurons from C57 black mice (DAPI,
450 blue fluorescence) were exposed to ZVBM peptides (FITC, green fluorescence) from (A) PRVABC59, (B)
451 MR_766, (C) IbH30656, and (D) PRVABC59 (scrambled). Punctate green staining around the DRG nuclei
452 was observed via laser confocal microscopy in panels A, B, and C, but was largely absent from panel D.

453

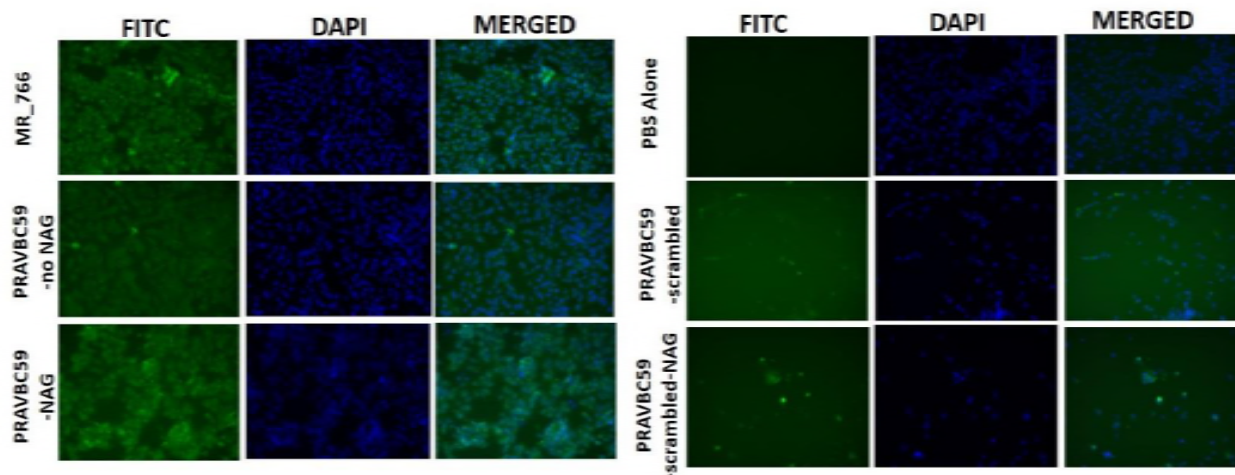
454 **Supplemental Material:**

455 Supplemental Table S1: ZIKV Adsorption Inhibition

Strain/Treatment	Mean TCID ₅₀	Significant Reduction?
ZIKV MR_766	9136667 ± 61191.3	--

ZIKV MR_766 + PRVABC59 ZVBM (no NAG)	1470000 ± 1895.2	Yes ($P<0.05$)
ZIKV MR_766	1085333 ± 66626.2	--
ZIKV MR_766 + PRVABC59 ZVBM (no NAG) - Scrambled	1288667 ± 89581.3	No
ZIKV PRVABC59	1920500 ± 1752918	--
ZIKV PRVABC59 + PRVABC59 ZVBM (NAG)	893666.7 ± 184175	Yes ($P<0.01$)
ZIKV PRVABC59	1470000 ± 2264	--
ZIKV PRVABC59 + PRVABC59 ZVBM (NAG) - Scrambled	473000 ± 18776	No
ZIKV PRVABC59	177033.3 ± 43766.67	--
ZIKV PRVABC59 + Annexin V	43766.67 ± 21073.28	Yes ($P<0.01$)
ZIKV MR_766	164866.7 ± 143039.3	--
ZIKV MR_766 + Annexin V	197366.7 ± 126649.5	No

456



457

458 **Supplemental Figure S1: Peptide binding to Vero Cells.** Vero cell monolayers (85% confluency) (DAPI,
 459 blue fluorescence) were exposed to ZVBM peptides (FITC, green fluorescence) from PRVABC59
 460 (NAGylated and unglycosylated), MR_766, and scrambled PRVABC59 peptides (NAGylated and
 461 unglycosylated). Co-localization of FITC and DAPI staining was observed for glycosylated and
 462 unglycosylated PRVABC59 and MR_766 peptides, but was largely absent from scrambled control
 463 peptides.

